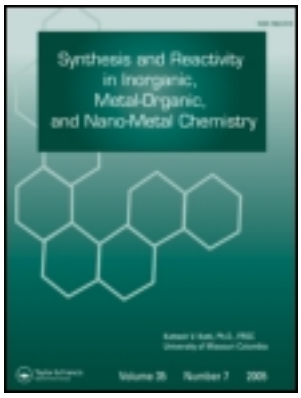

Synthesis and Reactivity in Inorganic, Metal-Organic, and Nano-Metal Chemistry

Publication details, including instructions for authors and subscription information:
http://www.tandfonline.com/loi/lsrt20

Lanthanide Complexes of 1-phenyl-3-methyl-5-hydroxypyrazole-4-carbaldehyde-(4′-hydroxybenzoyl) Hydrazone: Crystal Structure and Interaction Studies With Biomacromolecules

Ming-Fang Wang [a], Zheng-Yin Yang [a], Zeng-Chen Liu [a], Yong Li [a] & Hong-Ge Li [a]

[a] State Key Laboratory of Applied Organic Chemistry, College of Chemistry and Chemical Engineering, Lanzhou University, Lanzhou, P. R. China

Accepted author version posted online: 10 Dec 2012.

To cite this article: Ming-Fang Wang , Zheng-Yin Yang , Zeng-Chen Liu , Yong Li & Hong-Ge Li (2013) Lanthanide Complexes of 1-phenyl-3-methyl-5-hydroxypyrazole-4-carbaldehyde-(4′-hydroxybenzoyl) Hydrazone: Crystal Structure and Interaction Studies With Biomacromolecules, Synthesis and Reactivity in Inorganic, Metal-Organic, and Nano-Metal Chemistry, 43:4, 483-494, DOI: 10.1080/15533174.2012.740753

To link to this article: http://dx.doi.org/10.1080/15533174.2012.740753

Synthesis and Reactivity in Inorganic, Metal-Organic, and Nano-Metal Chemistry, 43:483–494, 2013

ISSN: 1553-3174 print / 1553-3182 online
DOI: 10.1080/15533174.2012.740753

Taylor & Francis
Taylor & Francis Group

Lanthanide Complexes of 1-phenyl-3-methyl-5-hydroxypyrazole-4-carbaldehyde-(4′-hydroxybenzoyl) Hydrazone: Crystal Structure and Interaction Studies With Biomacromolecules

Ming-Fang Wang, Zheng-Yin Yang, Zeng-Chen Liu, Yong Li, and Hong-Ge Li
State Key Laboratory of Applied Organic Chemistry, College of Chemistry and Chemical Engineering, Lanzhou University, Lanzhou, P. R. China

1-phenyl-3-methyl-5-hydroxypyrazole-4-carbaldehyde-(4′-hydroxybenzoyl) hydrazone and Ln(III) complexes have been synthesized and characterized. The interaction between these compounds and biomacromolecules was investigated by fluorescence and UV/vis absorption spectroscopy. The results suggested that the compounds caused fluorescence quenching of BSA through a static quenching procedure. Hydrophobic interaction force also played a major role in stabilizing the compounds. Moreover, interactions between calf thymus DNA and compound H_3L and its Ln(III) complexes were studied by spectroscopy and viscosity measurements. These studies showed that these compounds bind to DNA *via* an intercalation mode. Furthermore, antioxidant activities of compounds were determined by hydroxyl radical scavenging methods in detail.

Supplemental materials are available for this article. Go to the publisher's online edition of* Synthesis and Reactivity in Inorganic, Metal-Organic, and Nano-Metal Chemistry *to view the supplemental file.

Keywords antioxidant activity, bovine serum albumin, calf thymus DNA, crystal Schiff base, spectroscopy, structure

INTRODUCTION

In the past years, the interaction of small molecules with major biopolymers such as proteins and nucleic acid has caused much interest in the field of bioinorganic chemistry.[1–3] Among various biomacromolecules, serum albumins (SA) are the most abundant soluble proteins in the circulatory system of a wide variety of organisms.[4] Serum albumins possess many indispensable physiological functions, such as regulation of colloid osmotic pressure. And the most important property is that serum albumins served as a depot protein and a transport protein for many endogenous and exogenous compounds.[5,6] Bovine serum albumin (BSA) has been studied extensively due to its medical importance, stability, low cost, unusual ligand-binding properties, and special structural homology with human serum albumin (HSA).[7] BSA has two tryptophans, Trp-134 and Trp-212, embedded in the first subdomain IA and subdomain IIA, respectively. The primary binding site for most drugs on albumin is suggested to be close to the tryptophan residues 212 of the BSA, locating in subdomain IIA.[8] Deoxyribonucleic acid (DNA), as another kind of biomacromolecule, is an important genetic substance in organism. Moreover, DNA is the intracellular target for a wide range of anticancer and antibiotic drugs. So the binding studies of small molecules with DNA could provide useful information for finding sensitive DNA molecular probes and have important significance in developing potential drugs for clinical applications.[9–12]

The previously mentioned studies inspire considerable interests in the field of the biochemical behavior of the interaction between small molecules and BSA/DNA. Moreover, fluorescence spectroscopy is essentially a probe technique sensing changes in the local environment of fluorophore. Any possibilities of structural rearrangements may lead to a fluorescence signal. Then by analyzing the fluorescence parameters, much information about the structural changes can be obtained.[13,14] Fluorescence spectroscopy is an appropriate method to determine the interaction between the small molecules and biomacromolecules, so does the UV/vis spectroscopy.

It is well known that reactive oxygen species (ROS) are generated by normal cellular metabolism and exogenous agents. Under pathological conditions, ROS are overproduced and result in oxidative stress in living organism. ROS are generated when endogenous antioxidant defenses are inadequate.[15] Among all the ROS, hydroxyl radical ($HO^{\bullet}$) is a highly reactive product. It is involved in the pathogenesis of various diseases through direct effects on DNA and by acting as a tumor promoter.[16] Therefore elimination of this radical is one of the major aims of antioxidant administration.

Schiff bases are a vital class of ligands in coordination chemistry and are found to possess extraordinary bioactivities.

Received 29 March 2012; accepted 13 October 2012.
This work is supported by the National Natural Science Foundation of China (20975046) and (81171337).
Address correspondence to Zheng-Yin Yang, State Key Laboratory of Applied Organic Chemistry, College of Chemistry and Chemical Engineering, Lanzhou University, Lanzhou 730000, P. R. China. E-mail: yangzy@lzu.edu.cn

In addition, the bioactivities of lanthanide complexes such as antimicrobial, antitumor, antivirus, and antioxidant activity have been explored in recent decades.[17,18] Based on the previous considerations, lanthanide complexes with Schiff bases such as 1-Phenyl-3-methyl-4-benzoyl-5-pyrazolone (PMBP) and 1-Phenyl-3-methyl-4-formyl-5-pyrazolone (PMFP) have been a major concern in our group.[19,20] In this article, three lanthanide complexes with a new Schiff base, 1-phenyl-3-methyl-5-hydroxypyrazole-4-carbaldehyde-(4′-hydroxy-benzoyl)hydrazone, are synthesized. Their BSA and DNA interaction modes are investigated by fluorescence and UV/vis absorption spectra. Antioxidant properties of the ligand and its lanthanide complexes are also studied.

EXPERIMENTAL

Materials

All chemicals used were of analytical grade. Bovine serum albumin (BSA, Fraction V, essentially fatty acid free, approximately 99%) was purchased from the Kehao Biotechnology Company, China. BSA stock solution (3×10^{-6} M, based on its molecular weight of 68,000) was prepared in the Tris–HCl buffer solution and kept in the dark at 4°C. Tris–HCl buffer solution for BSA consists of Tris (0.2 M) and HCl (0.1 M), and the pH was adjusted to 7.4 by adding NaOH. NaCl (1.0 M) solution was used to maintain the ion strength at 0.1 M. Calf thymus (DNA) was purchased from Sigma Chemical Co. (USA). Solution of DNA in 5 mM Tris and 50 mM NaCl (pH = 7.2) gave ratios of UV absorbance of about 1.8–1.9:1 at 260 and 280 nm, indicating that the DNA was sufficiently free of protein.[21] The DNA concentration per nucleotide was determined spectrophotometrically by employing an extinction coefficient of 6600 M^{-1} cm^{-1} at 260 nm.[22] The double-distilled water was used throughout the experiments.

Physical Measurement

Carbon, hydrogen, and nitrogen were performed using an Elemental Vario EL analyzer (Germany). The metal contents of the complexes were determined by titration with EDTA (xylenol orange tetrasodium salt used as an indicator and hexamethylidynetetraimine as buffer). The melting point of the ligand was obtained on a Beijing XT4–100X microscopic melting point apparatus (China). The IR spectra were recorded in KBr discs on a Thermo Mattson FTIR spectrophotometer (USA) in the 4,000–400 cm^{-1} region. ^{1}H NMR spectra were recorded on a Varian VR 300MHz spectrometer (USA) in DMSO-d^6 (dimethyl sulfoxide) with TMS (tetramethylsilane) as an internal standard. Conductivity measurements were determined in DMF (N,N-dimethyl formamide) solution with a DDS-11C conductometer (Shanghai Analytical Instrument Factory, China) at 25.0°C. The UV/Vis spectra were taken on a Perkin–Elmer Lambda 35 UV/vis spectrophotometer (USA). Fluorescence emission spectra were obtained with a RF-5301PC spectrofluorophotometer (Shimadzu, Japan) equipped with a xenon lamp source and 1.0 cm quartz cells. An electronic thermo regulating water bath (NTT-2100, EYELA, Japan) was used to control the temperature of the samples. Viscosity experiments were conducted on an Ubbelodhe viscometer (China), immersed in a thermostated water-bath maintained at 25 ± 0.1°C. The antioxidant activities were performed in DMF with a 721-E spectrophotometer (Shanghai Analytical Instrument Factory, China).

Preparation of the Ligand (H_3L)

As shown in Figure 1, 1-phenyl-3-methyl-4-formyl-2-pyrazolin-5-one (PMFP) was prepared according to the

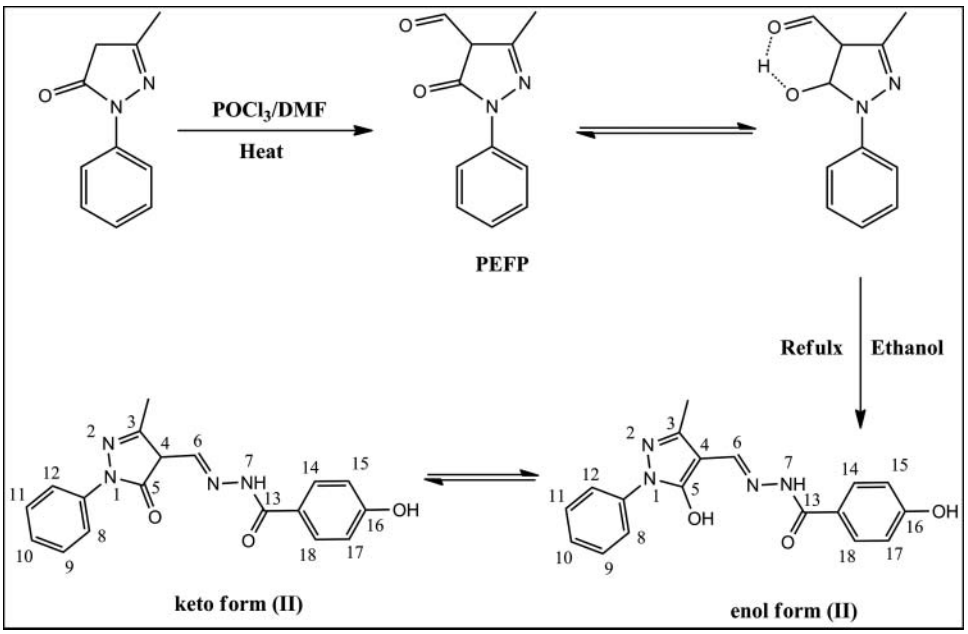

FIG. 1. The synthetic routes for ligand.

literature.[23,24] Synthesis of the ligand (H_3L) was in accordance with the following method: the ethanol solution (10 mL) contained 4-Hydroxybenzhydrazide (1.67 g, 11 mmol) was added dropwise to the PMFP (2.02 g, 10 mmol) dissolved in ethanol (20 mL) with stirring at 60°C for 3 h, then a large amount of yellow precipitate appeared. The yellow solid was filtered off and recrystallized from ethanol, then dried in a vacuum. Yield: 90% m.p. 281–282°C. IR νmax (cm^{-1}): $\nu(C_{(13)}{=}O)$:1656, ν (C=N): 1594, $\nu(C_{(5)}{=}O)$: 1533, ν(N–H): 3069 cm^{-1}. ^{1}H NMR (300 MHz, DMSO-d^6, ppm): 10.31 (s, 1H, H_{16}), 8.06 (s, 1H, H_7), 7.95 (dd, 2H, H_{14}, H_{18}, J = 5.4Hz, 16.8Hz), 7.82 (dd, 2H, H_{15}, H_{17}, J = 5.4Hz, 16.8Hz), 7.78 (d, 1H, H_{10}, J = 8.7Hz), 7.41 (m, 2H, H_9, H_{11}), 7.26 (s, 1H, H_6), 6.90 (dd, 2H, H_8, H_{12}, J = 13.2Hz, 8.7Hz), 2.18 (s, 3H, CH_3-pyrazole). The label numbers of H-atoms were shown in Figure 1.

Preparation of the Rare Earth Complexes

The ligand H_3L (0.35 mmol, 0.117 g) and the Eu(III) nitrate (0.2 mmol, 0.089 g) were added together in methanol (20 mL). The solution was refluxed on a water bath for 12 h with stirring and there was a yellow precipitate in the solution. The precipitate was separated from the solution by suction filtration, purified by washing several times with water, and dried in a vacuum. The Tb(III) and Dy(III) complexes were prepared by the same method. Anal. Calcd. for Eu(III) complex $C_{37}H_{34}N_9O_{10}Eu$: C, 48.48; H, 3.74; N, 13.75; Eu, 16.58. Found: C, 48.52; H, 3.66; N, 13.79; Eu, 16.70. IR ν_{max} (cm^{-1}): $\nu_{(13)C=O}$: 1612, $\nu_{C=N}$: 1571,$\nu_{(5)C=O}$: 1456, ν_{NO_3}: 1522, 1358, 1174, 818, $\nu_{M\text{-}O}$: 621, $\nu_{M\text{-}N}$: 424 cm^{-1}. U_{max} (nm): 351 nm. Λ_m (S cm^2 mol^{-1}): 36.6. Anal. Calcd. for Tb(III) complex $C_{36}H_{30}N_9O_9Tb$: C, 48.50; H, 3.39; N, 14.14; Tb, 17.82. Found: C, 48.52; H, 3.36; N, 14.28; Tb, 17.84. IR ν_{max} (cm^{-1}): $\nu_{(13)C=O}$: 1613, $\nu_{C=N}$: 1568,$\nu_{(5)C=O}$: 1455, ν_{NO_3}: 1520, 1357, 1174, 819, $\nu_{M\text{-}O}$: 621, $\nu_{M\text{-}N}$: 427 cm^{-1}. U_{max} (nm): 351 nm. Λ_m (S cm^2 mol^{-1}): 40.9. Anal. Calcd for Dy(III) complex $C_{36}H_{32}N_9O_{10}Dy$: C, 47.35; H, 3.53; N, 13.80; Dy, 17.79. Found: C, 47.52; H, 3.41; N, 13.85; Dy, 17.80. IR ν_{max} (cm^{-1}): $\nu_{(13)C=O}$: 1613, $\nu_{C=N}$: 1569,$\nu_{(5)C=O}$: 1457, ν_{NO_3}: 1521, 1357, 1145, 818, $\nu_{M\text{-}O}$: 621, $\nu_{M\text{-}N}$: 419 cm^{-1}. U_{max} (nm): 353 nm. Λ_m (S cm^2 mol^{-1}): 33.7.

X-Ray Crystal Structure Determination

A yellow crystal of Eu(III) complex was obtained by slow vapor diffusion of methanol/ether at room temperature. X-ray diffraction data for the crystal were performed with graphite-monochromated Mo-K radiation (0.71073 Å) on a Bruker APEX area-detector diffractometer (Germany) and collected by the $\omega/2\theta$ scan technique at 298(2) K. The crystal structure was solved by direct methods. The positions of non-hydrogen atoms were determined from successive Fourier syntheses. The hydrogen atoms were placed in their geometrically calculated positions. The positions and anisotropic thermal parameters of all non-hydrogen atoms were refined on F^2 by full-matrix least-squares techniques with the SHELX-97 program package.[25] Absorption correction was employed using semiempirical methods from equivalents.

Experimental Procedure

Binding mode between all compounds and BSA

Fluorometric titration experiments: 3.0 mL solution containing appropriate concentration of BSA was titrated manually by successive additions of stock solution of all compounds (to give a final concentration of 1.67×10^{-6} to 16.70×10^{-6} M) with trace syringes. Fluorescence experiments were performed at three different temperatures (292, 301, and 310 K). The fluorescence spectra from 290 to 500 nm of the above solution were collected with the excitation wavelength at 280 nm. The fluorescence is attributed to a tryptophan residue.[26] Fluorescence quenching was calculated using the well-known Scatchard's equation[27,28]:

$$r/D_f = nK - rK \quad [1]$$

Where r ($r = \Delta F / F_0$) represents the number of moles of bound small molecules per mole of protein, D_f represents the molar concentration of free drug, and n and K are the number of binding sites and binding constant, respectively. UV/vis absorption spectra were recorded by the same titration experiments at a constant room temperature.

DNA binding procedures

Electronic absorption titration experiments are performed with fixed concentration of drugs (1.0×10^{-6} M), with gradually increasing the concentration of DNA. When measuring the absorption spectra, an equal amount of DNA is added to both the sample and the reference solutions to eliminate the absorbance of DNA itself. To compare quantitatively the affinity of these compounds binding to DNA, the intrinsic binding constant (K_b) is estimated using the following equation through a plot of [DNA] / ($\varepsilon_a - \varepsilon_f$) vs. [DNA][29]:

$$[DNA]/(\varepsilon_a - \varepsilon_f) = [DNA]/(\varepsilon_b - \varepsilon_f) + 1/[K_b(\varepsilon_b - \varepsilon_f)] \quad [2]$$

Where [DNA] is the concentration of DNA in base pairs, ε_a, ε_f, and ε_b are the apparent extinction coefficient (A_{obsd}/[compound]), the extinction coefficient for free compound, and the extinction coefficient for the compound in the fully bound form, respectively. In plots of [DNA] / ($\varepsilon_a - \varepsilon_f$) versus [DNA], K_b is given by the ratio of the slope to the intercept.

Further support for the ligand and complexes binding to DNA *via* intercalation is given through the emission quenching experiment. A solution (2.0 mL) of 5 μM DNA and 0.4 μM EB (at saturating binding levels) was titrated by 2.5–35 μM the lanthanide complexes and ligand. The fluorescence spectra from 540 to 700 nm of the solution were collected with the excitation wavelength at 525 nm. Quenching data were analyzed according to the Stern−Volmer equation, which could be used

to determine the fluorescent quenching mechanism:

$$F_0/F = 1 + K_q[Q] \quad [3]$$

Where F_0 and F are the fluorescence intensity in the absence and presence of drug at [Q] concentration, respectively; K_q is the quenching constant; and [Q] is the quencher concentration. Plots of F_0/F versus [Q] appear to be linear and K_q depends on temperature.[30]

Viscosity experiments were conducted on an Ubbelodhe viscometer, immersed in a thermostated water bath maintained to 25.0 ± 0.1°C. Titrations were performed for the ligand and complexes (0.5–4 μM), and each compound was introduced into a DNA solution (5 μM) present in the viscometer. Data were analyzed as $(\eta/\eta_0)^{1/3}$ versus the ratio of the concentration of the compound and DNA, where η is the viscosity of DNA in the presence of the compound and η_0 is the viscosity of DNA alone.[31,32] Viscosities were calculated from the observed flow time of solutions containing DNA corrected for the flow time of buffer alone (t_0), $\eta = t - t_0$.

Antioxidant activity determination

In antioxidant activity experiments hydroxyl radical ($HO^{\bullet}$) in aqueous media was generated through the Fenton reaction. Solution of the test compounds was prepared with DMF. The reaction mixture contained 2.0 mL 0.15 M phosphate buffer (pH = 7.4), 1.0 mL 114 μM safranin, 1 mL 945 μM EDTA–Fe(II), 1 mL 3% H_2O_2, and 30 μL the test compound solution (the final concentration: $C_{i\,(i=1-6)}$ = 1.0, 2.0, 3.0, 4.0, 5.0, 6.0 μM). The sample without the test compound was used as the control. The reaction mixtures were incubated at 37°C for 60 min in a water bath. Absorbances (A_i, A_0, A_c) at 520 nm were measured. The scavenging ratio is defined as

$$\text{Suppression ratio}\,(\%) = [(A_i - A_0)/(A_c - A_0)] \times 100\% \quad [4]$$

Where A_i is absorbance in the presence of the test compound; A_0 is absorbance of the blank in the absence of the test compound; A_c is absorbance in the absence of the test compound, EDTA–Fe(II), and H_2O_2.

The antioxidant activity was expressed as the 50% inhibitory concentration (IC_{50}). IC_{50} values were calculated from regression lines where x was the test compound concentration in μM and y was percent inhibition of the test compounds.

RESULTS AND DISCUSSION

Characterization of Ligand and Complexes

The complexes are air-stable for extended periods and soluble in DMSO, DMF, methanol, and ethanol; slightly soluble in acetonitrile; and insoluble in water, acetone, and ethyl ether. The molar conductivities of the complexes are around 33.7–40.9 S cm^2 mol^{-1} in DMF solution, showing that the complexes are nonelectrolytes.[33]

The IR spectra of the complexes are similar and IR spectra usually provide a lot of valuable information on coordination reactions. All the spectra are characterized by vibrational bands mainly due to the C=O, C=N, M-O, M-N, and nitrate groups. $\nu_{(hydrazonic)C=O}$ and $\nu_{(carbonyl)C=O}$ vibrations of the free ligand appear at 1651 and 1537 cm^{-1}, respectively; whereas for the complexes these peaks shift to about 1613, 1456 cm^{-1}, $\Delta\nu_{(ligand\text{-}complexes)\ (hydrazonic)C=O}$ is equal to 38 cm^{-1}, $\Delta\nu_{(ligand\text{-}complexes)\ (carbonyl)C=O}$ is equal to 81 cm^{-1}, respectively. The big gap of $\Delta\nu_{(ligand\text{-}complexes)\ (carbonyl)C=O}$ suggests that the oxygen atoms of pyrazole ring may take part in coordination by the enol form. The band at 1594 cm^{-1} for the free ligand is assigned to $\nu_{C=N}$ stretch, which shifts to about 1569 cm^{-1} for the complexes, and $\Delta\nu_{(ligand\text{-}complexes)}$ is equal to 25 cm^{-1}. In the complexes, the band at 621 cm^{-1} or so are assigned to ν_{M-O}, demonstrating that the oxygen atoms of carbonyl have formed a coordinative bond with the rare earth ions. Weak bands at 424 cm^{-1} or so are assigned to ν_{M-N} in the complexes. These shifts and new bands further confirm that the nitrogen of the imino-group bonds to the rare earth ions.[34]

The absorption bands of the coordinated nitrates are observed at about 1521 (ν_{as}) and 818 (ν_s) cm^{-1}. The ν_3 (E′) free nitrates appear at 1384 cm^{-1} in the spectra of the rare earth complexes. In addition, the separation of the two highest frequency bands 1521 cm^{-1} and 1358 cm^{-1} resulting in $|\nu_4 - \nu_1|$ is approximately 163 cm^{-1}, and accordingly the coordinated nitrate group in the complex is a bidentate ligand. In order to make sure the precise structures of the complexes, the crystal structure of the Eu(III) complex is analyzed as follows.

The Eu(III) complex crystallized in the triclinic lattice with a space group P-1. Each unit cell contained two molecules (Z = 2). The X-ray diffraction data for $[Eu(H_2L)_2(NO_3)(CH_3OH)]$ are given in Table 1. Selected bond lengths and angles are summarized in Table 2. The crystal structure in Figure 2 shows that the composition of the Eu(III) complex is $[Eu(H_2L)_2(NO_3)(CH_3OH)]$. Eu ion is nine coordinated with two ligands, one methanol molecule, and one nitrate. Each ligand act as a tridentate ligand, binding to Eu atom through the nitrogen atom from –C=N– group of Schiff base, oxygen atoms from 1-phenyl-3-methyl-5-hydroxypyrazole-4-carbaldehyde unit and O=C–NH– of the 4-Hydroxybenzhydrazide side chain. The distances for C38–O51, C43–O4, and C29–O8, C201–O3 are 1.284 Å, 1.266 Å, 1.270 Å, and 1.263 Å, respectively, which are between the C–O (1.41–1.44 Å) and C=O (1.19–1.23 Å) distances,[35] suggesting that the oxygen atoms of pyrazole ring take part in coordination by the enol form. Besides the distances for C38–C31 and C43–C55 are 1.424 Å and 1.393 Å, respectively, which are between the C–C (1.47–1.53 Å) and C=C (1.32–1.38 Å) distances, demonstrating the previous conclusion. So the ligand (H_3L) displays in the enol form (I), in the action it losses one proton and acts as a tridentate chelating agent H_2L^{-1} coordinated to the ion in the solid state. The physical analytical results indicate that the crystal structure has a 1:2 metal to ligand stoichiometry, the reason for this might be attributed to the fact that the bonding effect of nitrate anion

TABLE 1
Crystal data and experimental data of Eu(III) complex

Sum formula	$C_{76}H_{72}Eu_2N_{18}O_{21}$
Formula weight	1877.46
Moiety formula	$2(C_{37}H_{33}EuN_9O_{10})C_2H_6O$
Crystal color	Yellow
Crystal size (mm)	0.35 × 0.32 × 0.21
Temperature (K)	296(2)
Wavelength (Å)	0.71073
Radiation	Mo Kα
Crystal system	Triclinic
Space group	P—1
Z	2
a (Å)	14.9536(13)
b (Å)	21.111(2)
c (Å)	22.440(2)
α (°)	89.800(2)
β (°)	89.7420(10)
γ (°)	69.5120(10)
Volume (Å^3)	6635.8(10)
D (Calc) (g/cm^3)	0.940
μ (mm^{-1})	0.523
F (000)	1896.0
$\theta_{min/max}$ (°)	2.08–27.49
Index ranges	$-19 \le h \le 19$
	$-23 \le k \le 27$
	$-29 \le l \le 28$
Reflections collected	30459
Independent reflections	12949 ($R_{int} = 0.0635$)
Refinement method	Full matrix least-squares on F^2
Data/restraints/parameters	3900/51/1036
Goodness-of-fit on F^2	1.093
Final R indices [$I>2\sigma$ (I)]	$R_1 = 0.0864$, $\omega R_2 = 0.2702$
R indices (all data)	$R_1 = 0.1999$, $\omega R_2 = 0.3292$

TABLE 2
Selected bond lengths (Å) and angles (°) for Eu(III) complex

Bond name	Bond length	Bond name	Bond angle
Eu1–O51	2.284(7)	O51–Eu1–O4	95.9(3)
Eu1–O4	2.318(8)	O51–Eu1–O117	76.9(2)
Eu1–O117	2.409(7)	O4–Eu1–O117	134.9(2)
Eu1–O1B	2.425(8)	O51–Eu1–O1B	145.9(2)
Eu1–O11	2.433(7)	O4–Eu1–O1B	82.2(3)
Eu1–O5	2.531(8)	O117–Eu1–O1B	80.6(3)
Eu1–O2	2.576(8)	O51–Eu1–O11	135.1(2)
Eu1–N10	2.595(9)	O4–Eu1–O11	75.4(3)
Eu1–N9	2.610(8)	O117–Eu1–O11	139.2(3)
Eu2–N11	2.630(10)	O1B–Eu1–O11	77.7(3)
Eu2–O8	2.304(7)	O51–Eu1–O5	77.1(3)
Eu2–O3	2.319(8)	O4–Eu1–O5	146.8(2)
Eu2–O6	2.415(7)	O117–Eu1–O5	75.8(2)
Eu2–O10	2.442(7)	O1B–Eu1–O5	121.5(3)
Eu2–O41	2.443(8)	O11–Eu1–O5	86.7(3)
Eu2–O7	2.550(8)	O51–Eu1–O2	120.9(3)
Eu2–O23	2.584(8)	O4–Eu1–O2	142.2(3)
Eu2–N14	2.618(8)	O117–Eu1–O2	68.3(3)
C38–C31	1.424(13)	O1B–Eu1–O2	72.2(3)
C38–O51	1.284(12)	O11–Eu1–O2	72.3(3)
C26–O11	1.257(12)	O5–Eu1–O2	49.5(3)
C43–O4	1.266(13)	O51–Eu1–N10	71.3(3)
C43–C55	1.393(15)	O4–Eu1–N10	72.1(3)
C49–O117	1.247(12)	O117–Eu1–N10	63.3(3)
C29–C41	1.480(15)	O1B–Eu1–N10	75.8(3)
C29–O8	1.270(11)	O11–Eu1–N10	140.2(3)
C32–O10	1.269(12)	O5–Eu1–N10	132.6(3)
C201–O3	1.263(13)	N10–Eu1–N9	127.5(3)
C201–C52	1.383(15)		
C37–O6	1.236(12)		

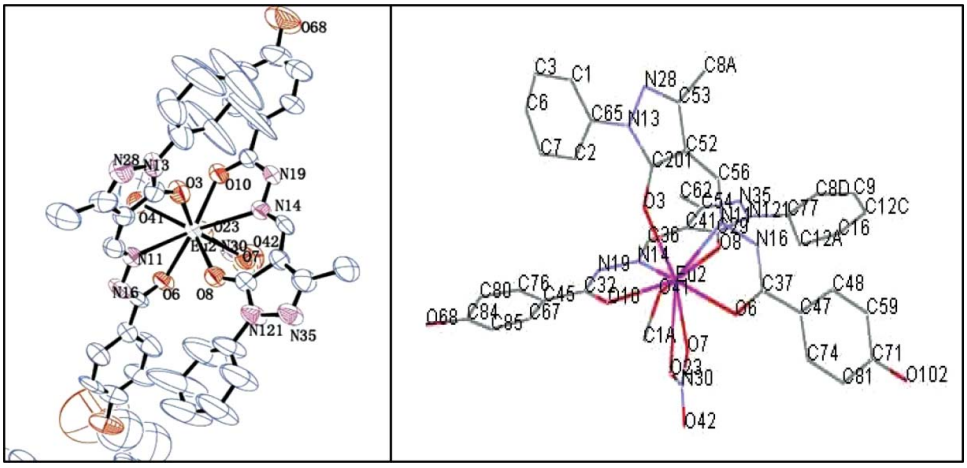

FIG. 2. The molecular structure of Eu(III) complex (color figure available online).

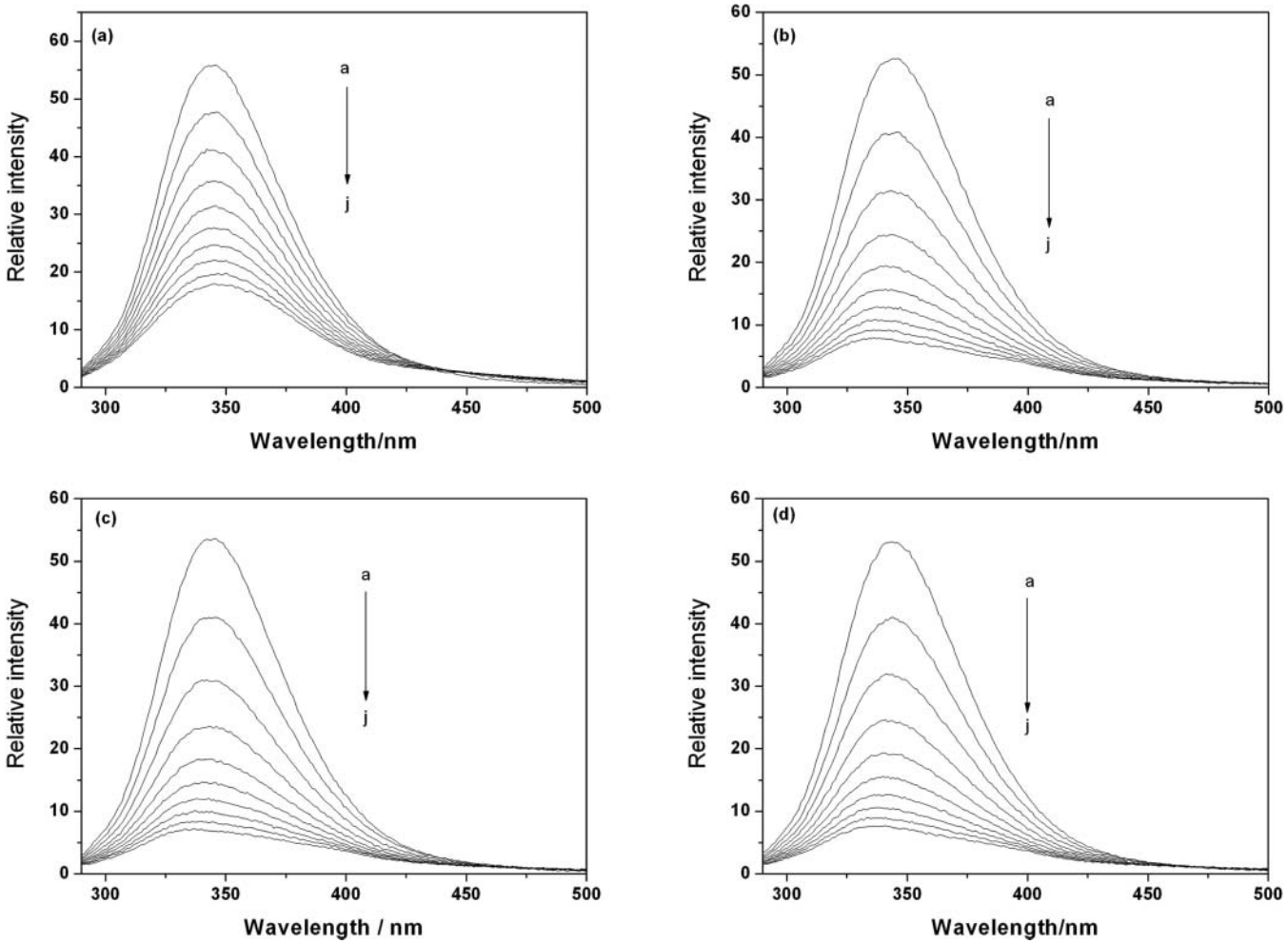

FIG. 3. Fluorescence spectra of BSA in the present of the ligand (a), Eu(III) (b), Tb(III) (c) and Dy(III) (d) complexes at 293K, pH = 7.40, c(BSA) = 3×10^{-6} M, c(compounds): 0, 1.67, 3.33, 5, 6.67, 8.33, 10, 11.67, 13.33, 15, 16.7×10^{-6} M.

with the metal ions are stronger than the ligand. Another reason may be that the coordination modes are different and the final complexes tend to form the most stable compound.

Binding Mode Between All Compounds and BSA

The effect of the ligand and its Ln(III) complex on BSA fluorescence intensity is shown in Figure 3. When BSA is titrated with different amounts of complexes, a remarkable intrinsic fluorescence decrease of BSA is observed. Figure 4 displays the Scatchard plots of the quenching of BSA fluorescence in the presence of the ligand and Ln(III) complex.

As reported, there are essentially four types of noncovalent interactions that could play a role in small molecules binding to proteins. These are hydrogen bonds, van der Waals forces, electrostatic, and hydrophobic interaction.[36] In order to elucidate the interaction between each compound and BSA, the thermodynamic parameters are calculated from the Van 't Hoff plots.[37] The values of ΔH and ΔS are obtained from the slope and intercept of linear Van 't Hoff plot, according to the Van 't Hoff equation:

$$\mathrm{In}K = \frac{-\Delta H}{RT} + \frac{\Delta S}{R} \qquad [5]$$

Where K is the binding constant at absolute temperature T and R is gas constant. The free energy change (ΔG) is then estimated from the following relationship:

$$\Delta G = \Delta H - T\Delta S \qquad [6]$$

On the basis of the binding constants obtained at the three previous temperatures, the thermodynamic parameters are determined and summarized in Table 3. The binding process is always spontaneous, as evidenced by the negative sign of ΔG values.[38]

According to the theory of Ross et al.,[39] for typical hydrophobic interactions, both enthalpy change (ΔH) and entropy change (ΔS) are positive, while the negative values of ΔH and ΔS are associated with hydrogen binding and van der Waals

TABLE 3
Binding parameters and thermodynamic parameters of the ligand–BSA and the complexes—BSA

	T (K)	K ($10^5 M^{-1}$)	n	ΔG° (kJ·mol^{-1})	ΔS° (J·mol^{-1}·K^{-1})	ΔH° (kJ·mol^{-1})
	292	0.8393	1.328	–23.673		
Ligand	301	0.8023	1.331	–24.403	81.061	–3.845
	310	0.7654	1.322	–25.133		
	292	2.017	1.173	–20.571		
Eu(III) complex	301	1.739	1.222	–21.205	70.419	–9.062
	310	1.165	1.234	–21.839		
	292	2.065	1.191	–19.044		
Tb(III) complex	301	1.757	1.221	–19.630	56.119	–13.335
	310	1.502	1.285	–20.217		
	292	1.848	1.223	–16.400		
Dy(III) complex	301	1.633	1.254	–16.905	65.182	–10.407
	310	1.441	1.275	–17.410		

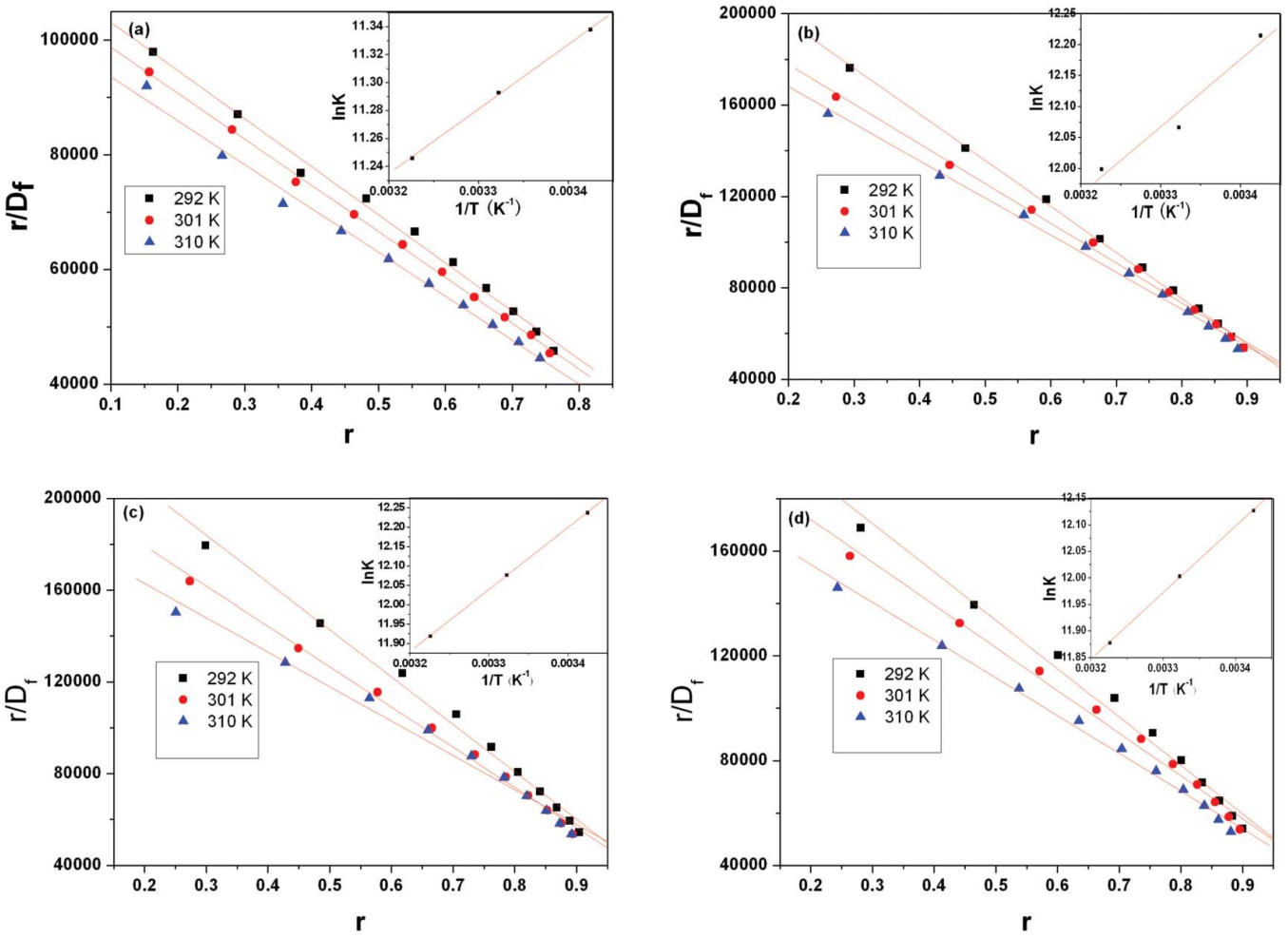

FIG. 4. The Scatchard plot for the binding of the ligand (a), Eu(III) (b), Tb(III) (c), and Dy(III) (d) complexes (pH = 7.40). The insert shows Van 't Hoff plot for the interaction of BSA and the compounds (color figure available online).

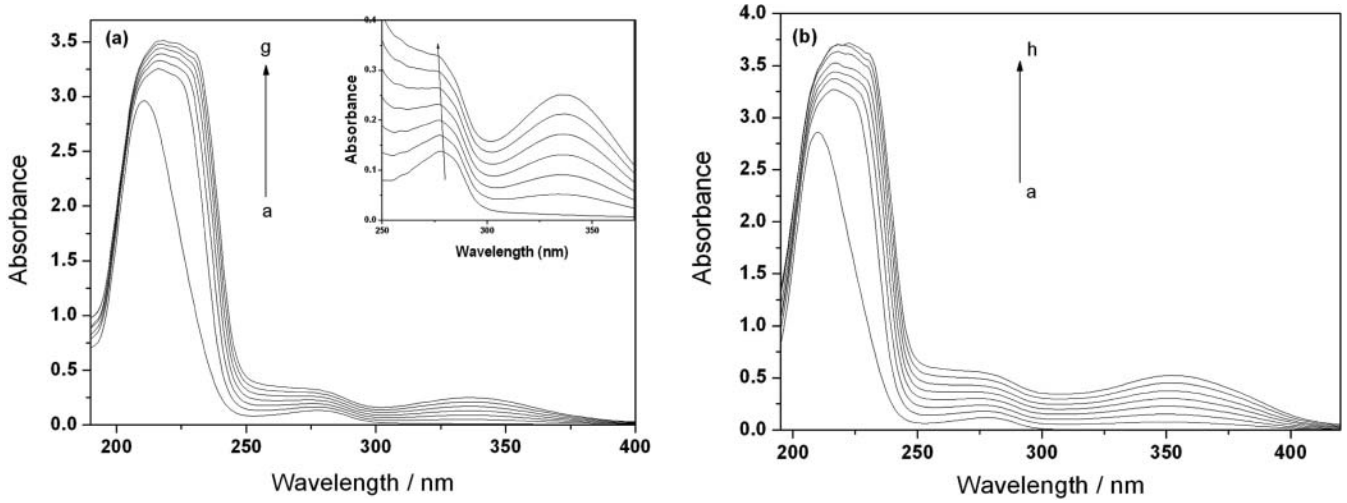

FIG. 5. UV/vis absorbance spectra of BSA in the presence of the ligand (a) and Eu(III) complex (b) at pH = 7.40, a–h, c(BSA) = 3.0×10^{-6} M; c(compounds): 0, 1.67, 3.33, 5, 6.67, 8.33, 10, 11.67, 13.33, 15, 16.7×10^{-6} M. The insert shows the UV/vis absorbance spectra ranging from 250 to 370 nm and arrow shows the absorbance changes with a blue shift upon increasing compounds concentration.

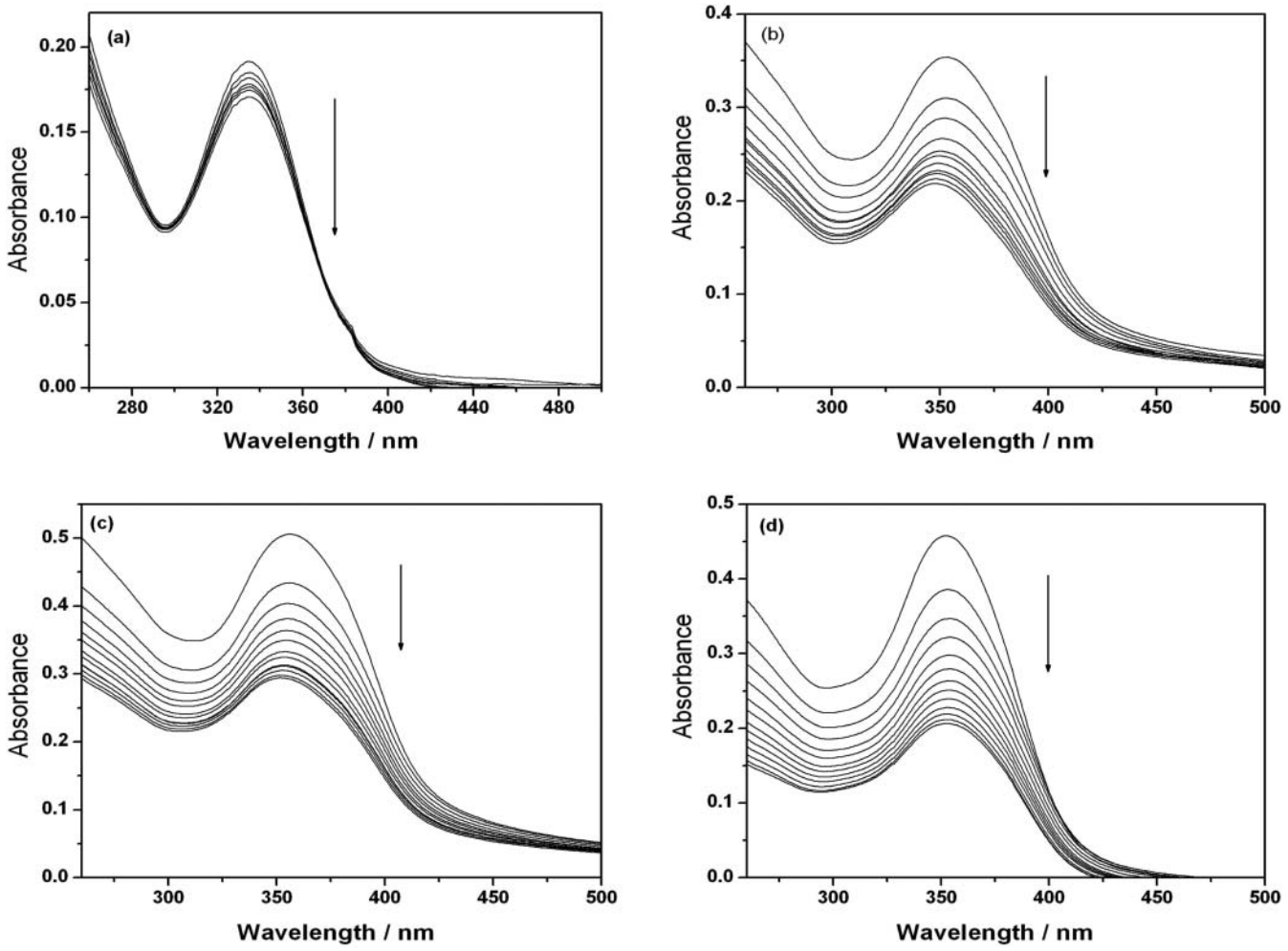

FIG. 6. Electronic absorption spectra of the ligand (a), Eu(III) (b), Tb(III) (c), and Dy(III) (d) complexes in the absence (top spectrum) and presence of increasing amounts of DNA (2.5, 5.0, 7.5, 10.0, 12.5, 15.0, 17.5, 20.0 and 22.5×10^{-6} M; subsequent spectra). The arrow shows the absorbance changes upon increasing DNA concentration.

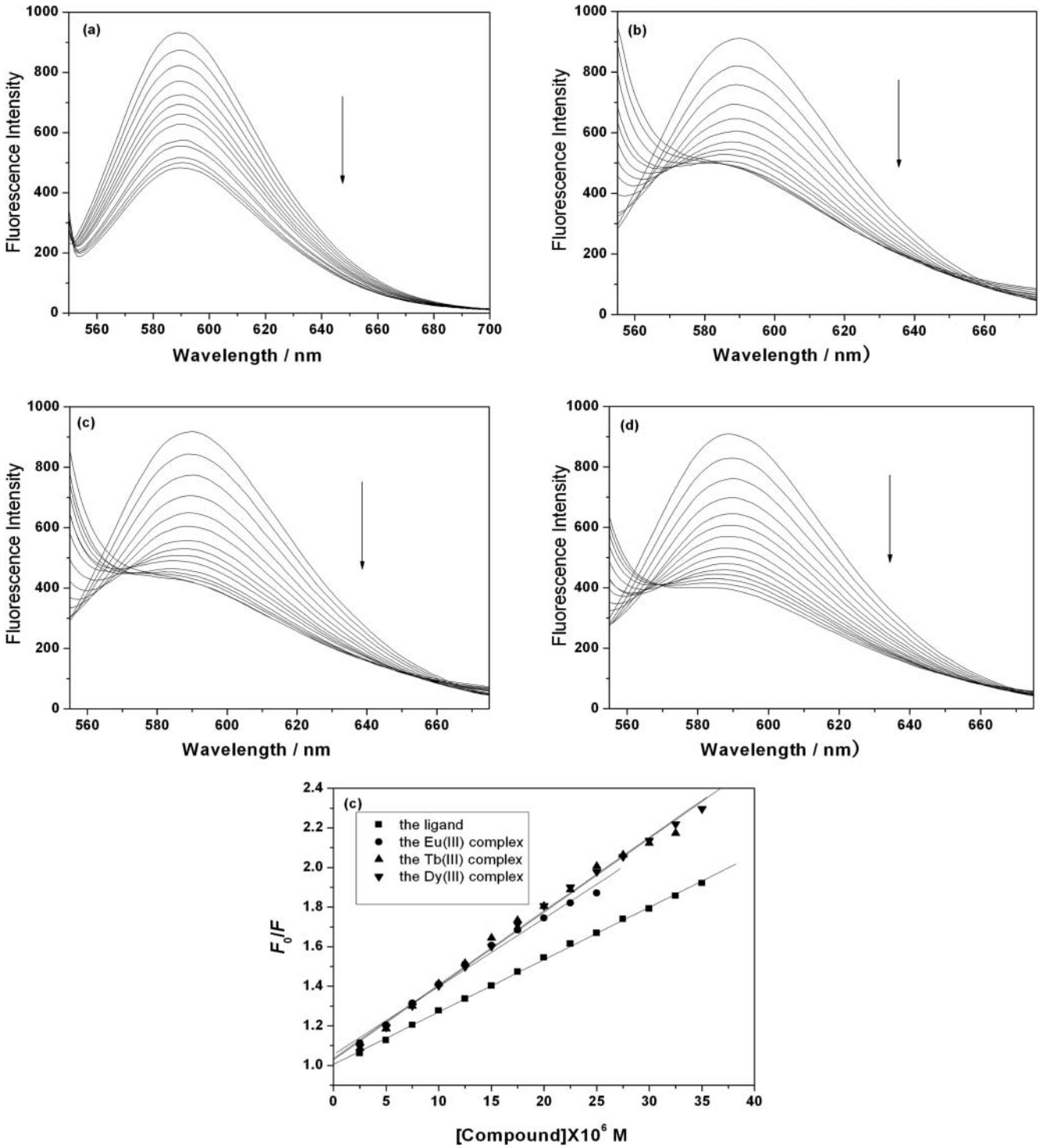

FIG. 7. The emission spectra of DNA-EB system $\lambda_{ex} = 525$ nm, in the presence of 0, 2.5, 5, 7.5, 10, 12.5, 15, 17.5, 20.0, 22.5, 25, 27.5, 30.0, 32.5, and 35.0 μM ligand (a), Eu(III) (b), Tb(III) (c), and Dy(III) (d) complexes. Arrow shows the emission intensity changes upon increasing ligand and complexes. (c) Plot of F_0/F versus [Q] for the titration of all compounds with DNA-EB.

interactions; finally, the very low positive or negative ΔH and positive ΔS values are characterized by electrostatic interactions.[40] As shown in Table 3, ΔH and ΔS have a small negative value and a large positive value, respectively. The main source of ΔG value is derived from a large contribution of ΔS term with little contribution from the ΔH factor, namely the binding process is entropy driven. It is more likely hydrophobic interaction is involved in the binding process.

For reconfirming the binding properties with BSA by the addition of the complexes, the UV/vis absorbance spectroscopy is employed. Figure 5 displays that the absorption intensity of BSA increases regularly with increasing concentration of the ligand and Eu(III) complex. The absorption band of 210 nm is characteristic of α-helix structure of BSA and around 280 nm is mainly due to the presence of tryptophan residues. Further, the blue shifts in absorption maximum around 280 nm indicate the changes in polarity around tryptophan residue and changes in the peptide strand of BSA molecule,[41,42] indicating effect occurred between the two substances.

DNA Binding Properties

Electronic absorption spectroscopy is one of the most universal techniques in DNA binding studies of compounds. Electronic absorption spectra of the ligand and its lanthanide complexes in the absence and presence of DNA (at a constant concentration of the compounds) are obtained (Figure 6). From the figure, we could obtain the relation that with increasing DNA concentrations the absorption bands showed hypochromism. In general, the reason these spectral characteristics are the strong stacking interaction between an aromatic chromophore and the base pairs of DNA, suggesting that the compounds may bind to DNA by an intercalative mode.[43] After intercalating the base pairs of DNA, the π^* orbital of the intercalated ligand could couple with π orbit of base pairs, thus, decreasing the π–π^* transition energy, and further resulting in the bathochromism. On the other hand, the coupling π^* orbital was partially filled by electrons, decreasing the transition probabilities, and concomitantly resulting in the hypochromism.[44] K_b values of the ligand, Eu, Tb, and Dy complexes are $7.72 \times 10^4\ M^{-1}$, $1.20 \times 10^5\ M^{-1}$, $1.22 \times 10^5\ M^{-1}$, and $1.04 \times 10^5\ M^{-1}$, respectively. These results show that the ligand and its Ln(III) complexes can bind to DNA, especially the Tb(III) complex binds more strongly than the free ligand.

EB (a typical indicator of intercalation) quenching assay is performed to further confirm the binding mode and compare their binding affinities. The emission spectra of EB bound to DNA in the absence and in the presence of the ligand and Eu(III) complex are given in Figure 7. The emission band at 589 nm of the DNA-EB system decreases in fluorescence intensity upon addition of every compound at diverse r (= [Compound]/[DNA]) values indicating that the competition of the compounds with EB in binding to DNA. The observed quenching of DNA-EB fluorescence intensity for the compounds suggests that they displace EB from the DNA-EB system and they can interact with DNA probably via the intercalative mode. The

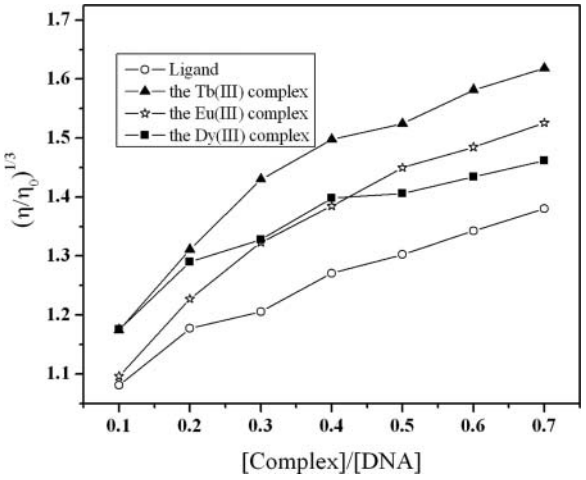

FIG. 8. Effects of increasing amounts of the ligand and its lanthanide complexes on the relative viscosity of CT DNA at 25.0 ± 0.1°C.

quenching constants K_q are used to evaluate the quenching efficiency discussed by Stern-Volmer's equation. The K_q values of the ligand, Eu, Tb, and Dy complexes are $2.646 \times 10^4\ M^{-1}$, $3.445 \times 10^4\ M^{-1}$, $3.725 \times 10^4\ M^{-1}$, and $3.726 \times 10^4\ M^{-1}$, respectively. The data show that the interaction of the Ln(III) complexes with DNA is stronger than that of the free ligand, which is consistent with the electronic absorption spectral results.

The effects of the ligand and its Ln(III) complexes on the viscosity of DNA are shown in Figure 8. The relative viscosities of DNA increase steadily with increasing concentrations of the compounds. The increased degree of viscosity depends on the binding affinity of the compounds to DNA. Viscosity measurements clearly show that all the compounds can intercalate between adjacent DNA base pairs, causing an extension in the helix and thus increase the viscosity of DNA, and the complexes can intercalate more strongly and deeply than the free ligand.

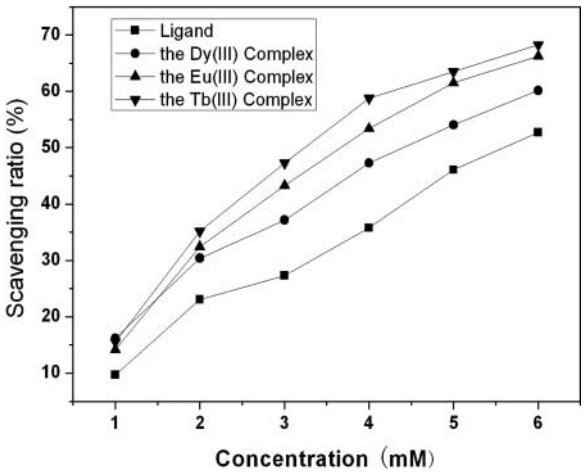

FIG. 9. Scavenging effects of the ligand and its lanthanide complexes on HO•.

TABLE 4
The influence of investigated compounds for HO•

Compound	Average inhibition (%) for HO· (μM) 1.0	2.0	3.0	4.0	5.0	6.0	Equation	IC_{50} (μM)	R^2
H_2L	9.70	23.03	27.27	35.76	46.06	52.73	y = 53.25x + 7.06	6.40	0.973
Dy(III) Complex	16.22	30.41	37.16	47.30	54.05	60.14	y = 55.86x + 14.27	4.36	0.990
Eu(III) Complex	14.19	32.43	43.24	53.38	61.49	66.22	y = 67.63x + 12.95	3.53	0.998
Tb(III) Complex	15.54	35.14	47.30	58.78	62.16	68.24	y = 68.43x + 15.27	3.22	0.998

IC_{50} values were calculated from regression lines where x was log of the tested compound concentration and y was percent inhibition of the tested compounds. When the percent inhibition of the tested compounds was 50%, the tested compound concentration was IC_{50}. R^2 = correlation coefficient.

The results obtained from the viscosity validate those obtained from the spectroscopic studies.

Antioxidant Activity Determination

Because the synthesized ligand and its rare earth complexes exhibit good binding affinity with biomacromolecule it is considered worthwhile to investigate their other biological activities, such as antioxidant activity. In this paper, the antioxidant activity of the ligand and its rare earth complexes is studied by comparing their scavenging effects on hydroxyl radical (HO•).

The data of the suppression ratio for HO• are listed in Table 4. IC_{50} values for the ligand and complexes are 6.40 and 3.22–4.36 μM, respectively (Figure 9). The inhibitory effect of the compounds is marked and the average suppression ratio for HO• increases with the increasing compound concentration. The average suppression ratio of the lanthanide complexes is higher than the ligand and this is due to the chelation of organic molecules to lanthanide ions, which can exert differential and selective effects on scavenging radicals of the biological system. It is reported that IC_{50} value of ascorbic acid (Vc, a standard agent for nonenzymatic reaction) for HO• is 1.537 mg mL^{-1} (8.727 mmol),[45] notably, the investigated ligand and lanthanide complexes have much stronger scavenging abilities for HO• radical than the standard antioxidant (vitamin C).

CONCLUSION

This article reports a new ligand 1-phenyl-3-methyl-5-hydroxypyrazole-4-carbaldehyde-(4′-hydroxybenzoyl) hydrazone (H_3L) and its Ln(III) complexes. The structure of [Eu(H_2L)(NO_3)(CH_3OH)] was determined by single crystal X-ray diffraction. Interactions between these compounds with BSA/DNA have been studied by UV/vis and fluorescence spectroscopy. On one hand, the binding process of these compounds on BSA was a spontaneous molecular interaction procedure in which entropy increased and Gibbs free energy decreased. From the thermodynamic analysis, it was shown that the acting force was mainly hydrophobic interactions. On the other hand, the metal complexes could bind to DNA and remarkably quench the emission intensity of the DNA-EB system. Experimental results indicate that the ligand and the complexes bond to DNA by an intercalation mode. Additionally, both the ligand and the complexes have some antioxidant properties of scavenging hydroxyl radicals. The complexes show stronger scavenging effects than the ligand. The binding study of inorganic compounds with proteins and nucleic acid is of great importance in pharmacy, pharmacology and biochemistry. Information obtained from this work may be helpful to the development of biomacromolecule probes and new therapeutic reagents for some diseases. Further investigations on the pharmacodynamics and physiology should be lucubrated.

REFERENCES

1. McMillin, D.R.; McNett, K.M. Photoprocesses of copper complexes that bind to DNA. *Chem. Rev.* **1998**, *98*, 1201–1219.
2. Baldini, M.; Belicchi-Ferrari, M.; Bisceglie, F.; Pelosi, G.; Pinelli, S.; Tarasconi, P. Cu(II) complexes with heterocyclic substituted thiosemicarbazones: the case of 5-formyluracil. Synthesis, characterization, x-ray structures, DNA interaction studies, and biological activity. *Inorg. Chem.* **2003**, *42*, 2049–2055.
3. Zeglis, B.M.; Barton, J.K. Binding of $Ru(bpy)_2(eilatin)^{2+}$ to matched and mismatched DNA. *Inorg. Chem.* **2008**, *47*, 6452–6457.
4. Liu, Y.F.; Xu, X.Y.; Xia, H.T.; Wang, D.Q.; Liu, H. Synthesis, crystal structure and bovine serum albumin interaction studies of a binuclear copper(II) complex with naphthylacetic acid. *Synth. React. Inorg. Met.-Org. Nano-Met. Chem.* **2009**, *39*, 400–405.
5. Guo, Y.M.; Yue, Q.Y.; Gao, B.Y.; Zhong, Q.Q. Spectroscopic studies on the interaction between disperse blue SBL and bovine serum albumin. *J. Luminesc.* **2010**, *130*, 1384–1389.
6. Malonga, H.; Neault, J.F.; Tajmir-Riahi, H.A. Transfer RNA binding to human serum albumin: A model for protein-RNA interaction. *DNA Cell Biol*. **2006**, *25*, 393–398.
7. Shahabadi, N.; Maghsudi, M.; Kiani, Z.; Pourfoulad, M. Multispectroscopic studies on the interaction of 2-tert-butylhydroquinone (TBHQ), a food additive, with bovine serum albumin. *Food Chem.* **2011**, *124*, 1063–1068.
8. Ni, Y.N.; Liu, C.L.; Kokot, S. Fluorescence spectrometric study on the interactions of Isoprocarb and sodium 2-isopropylphenate with bovine serum albumin. *Talanta* **2008**, *76*, 513–521.
9. Pyle, A.M.; Morri, T.; Barton, J.K. Probing microstructures in double-helical DNA with chiral metal complexes: recognition of changes in base-pair propeller twisting in solution. *J. Am. Chem. Soc.* **1990**, *112*, 9432–9434.
10. Purmal, A.A.; Shabarv, T.V.; Gumport, R.I. A new affinity reagent for the site-specific, covalent attachment of DNA to active-site nucleophiles: application to the EcoRI and Rsrl restriction and modification enzymes. *Nucleic Acid Res.* **1992**, *20*, 3713–3719.

11. Trawick, B.N.; Daniher, A.T.; Bashkin, J.K. Inorganic mimics of ribonucleases and ribozymes: from random cleavage to sequence-specific chemistry to catalytic antisense drugs. *Chem. Rev.* **1998**, *98*, 939–960.
12. Wu, S.S.; Yuan, W.B.; Wang, H.Y.; Zhang, Q.; Liu, M.; Yu, K.B. Synthesis, crystal structure and interaction with DNA and HSA of (N,N'-dibenzylethane-1,2-diamine) transition metal complexes. *J. Inorg. Biochem.* **2008**, *102*, 2026–2034.
13. Wang, Y.P.; Wei, Y.L.; Dong, C.; Wang, T.H.; Zhao, Z.M. Study on the interaction of 3,3-bis(4-hydroxy-1-naphthyl)-phthalide with bovine serum albumin by fluorescence spectroscopy. *J. Photochem. Photobiol. A* **2006**, *177*, 6–11.
14. Wang, T.H.; Zhao, Z.M.; Wei, B.Z.; Zhang, L.; Ji, L. Spectroscopic investigations on the binding of dibazol to bovine serum albumin. *J. Mol. Struct.* **2010**, *970*, 128–133.
15. Gülcin, İlhami. Antioxidant and antiradical activities of L-Carnitine. *Life Sci.* **2006**, *78*, 803–811.
16. Leonard, S.S.; Keil, D.; Mehlmanb, T.; Proper, S.; Shi, X.; Harris, G.K. Essiac tea: scavenging of reactive oxygen species and effects on DNA damage. *J. Ethnopharmacol.* **2006**, *103*, 288–296.
17. Albrecht, M.; Osetska, O.; Fröhliich, R. 2-[(8-Hydroxyquinolinyl)methyl ene] hydrazinecarboxamide: expanding the coordination sphere of 8-hydroxyquinoline for coordination of rare-earth metal(III) ions. *Dalton Trans.* **2005**, *23*, 3757–3762.
18. Li, Y.; Yang, Z.Y.; Wang, M.F. Synthesis, characterization, DNA binding properties and antioxidant activity of Ln(III) complexes with hesperetin-4-one-(benzoyl) hydrazone. *Eur. J. Med. Chem.* **2009**, *44*, 4585–4595.
19. Yang, Z.Y.; Wang, B.D.; Li, Y.H. Study on DNA-binding properties and cytotoxicity in L_{1210} of La(III) complex with PMBP-isonicotinoyl hydrazone. *J. Organomet. Chem.* **2006**, *691*, 4159–4166.
20. Li, H.G.; Yang, Z.Y.; Wang, B.D.; Wu, J.C. Synthesis, crystal structure, antioxidation and DNA-binding properties of the Ln complexes with 1-phenyl-3-methyl-5-hydroxypyrazole-4-carbaldhyde-(benzoyl)hydrazone. *J. Organomet. Chem.* **2010**, *695*, 415–422.
21. Satyanaryana, S.; Dabrowiak, J.C.; Chaires, J.B. Tris(phenanthroline) ruthenium(II) enantiomer interactions with DNA: mode and specificity of binding. *Biochemistry* **1993**, *32*, 2573–2584.
22. Marmur, J. A procedure for the isolation of deoxyribonucleic acid from micro-organisms. *J. Mol. Biol.* **1961**, *3*, 208–218.
23. Wallace, D.J.; Straley, J.M. Synthesis of 5-Oxo-2-pyrazoline-4-carboxaldehyde. *J. Org. Chem.* **1961**, *26*, 3825–3826.
24. Li, H.G.; Yang, Z.Y.; Qin, D.D. A new Schiff-base type selective fluorescent chemosensor for Cu^{2+}. *Inorg. Chem. Commun.* **2009**, *12*, 494–497.
25. Sheldrick, G.M. *SHELXTL*, *Version 6.12*; Bruker AXS Inc., Madison, WI, USA, **2001**.
26. Pan, B.F.; Gao, F.; Ao, L.M. Investigation of interactions between dendrimer-coated magnetite nanoparticles and bovine serum albumin. *J. Magn. Magn. Mater.* **2005**, *293*, 252–258.
27. Eftink, M.R. Biophysical and biochemical aspects of fluorescence spectroscopy. In *Fluorescence Quenching Reactions: Probing Biological Macromolecular Structures*, T.G. Eewey, ed.; Plenum Press, New York, **1991**, vol. 5, pp. 1–41
28. Scatchard, G. The attractions of proteins for small molecules and ions. *Ann. N. Y. Acad. Sci.* **1949**, *51*, 660–672.
29. Wolfe, A.; Shimer, G.H.; Meehan, T. Polycyclic aromatic hydrocarbons physically intercalateinto duplex regions of denatured DNA. *Biochemistry* **1987**, *26*, 6392–6396.
30. Eftink, M.R.; Ghiron, C.A. Fluorescence quenching studies with proteins. *Anal Biochem.* **1981**, *114*, 199–227.
31. Eriksson, M.; Leijon, M.; Hiort, C.; Norden, B.; Graeslund, A. Binding of Δ– and Λ–$[Ru(phen)_3]^{2+}$ too $[d(CGCGATCGCG)]_2$ studied by NMR. *Biochemistry* **1994**, *33*, 5031–5040.
32. Xiong, Y.; He, X.F.; Zou, X.H.; Wu, J.Z.; Chen, X.M.; Ji, L.N.; Li, R.H.; Zhou, J.Y.; Yu, K.B. Interaction of polypyridyl ruthenium(II) complexes containing non–planar ligands with DNA. *J. Chem. Soc., Dalton Trans.* **1999**, *1*, 19–24.
33. Geary, W.J. The use of conductivity measurements in organic solvents for the characterisation of coordination compounds. *Coord. Chem. Rev.* **1971**, *7*, 81–122.
34. Marchetti, F.; Pettinari, C.; Pettinari, R.; Cingolani, A.; Leonesi, D.; Lorenzotti, A. Group 12 metal complexes of tetradentate N_2O_2-Schiff-base ligands incorporating pyrazole: synthesis, characterisation and reactivity toward S-donors, N-donors, copper and tin acceptors. *Polyhedron* **1999**, *18*, 3041–3050.
35. Chen, X.M.; Cai, J.W. eds. *Single-Crystal Structural Analysis. Principles and Practices*; Science Press, Beijing, **2003**.
36. Klotz, I.M. Physiochemical aspects of drug-protein interactions: a general perspective. *Ann. N. Y. Acad. Sci.* **1973**, *226*, 18–35.
37. Timaseff, S.N. Thermodynamics of protein interactions. In *Proteins of Biological Fluids*, H. Peeters, ed.; Pergamon Press, Oxford, **1972**, pp. 511–519.
38. Tian, J.N.; Liu, J.Q.; He, W.Y.; Hu, Z.D.; Yao, X.J.; Chen, X.G. Probing the binding of scutellarin to human serum albumin by circular dichroism, fluorescence spectroscopy, FTIR, and molecular modeling method. *Biomacromolecules*, **2004**, *5*, 1956–1961.
39. Ross, P.D.; Subramanian, S. Thermodynamics of protein association reactions: Forces contributing to stability. *Biochem.* **1981**, *20*, 3096–3102.
40. Shi, X.L.; Li, X.W.; Gui, M.Y.; Zhou, H.Y.; Yang, R.J.; Zhang, H.Q.; Jin, Y.R. Studies on interaction between flavonoids and bovine serum albumin by spectral methods. *J. Luminesc.* **2010**, *130*, 637–644.
41. Ulrich, K.H. Molecular aspects of ligand binding to serum albumin. *Pharmacol. Rev.* **1981**, *33*, 17–53.
42. Hu, Y.J.; Liu, Y.; Wang, J.B.; Xiao, X.H.; Qu, S.S. Study of the interaction between monoammonium glycyrrhizinate and bovine serum albumin. *J. Pharma. Biomed. Anal.* **2004**, *36*, 915–919.
43. Hecht, S.M. Bleomycin: new perspectives on the mechanism of action. *J. Nat. Prod.* **2000**, *63*, 158–168.
44. Pyle, A.M.; Rehmann, J.P.; Meshoyrer, R.; Kumar, C.V.; Turro, N.J.; Barton, J.K. Mixed–ligand complexes of ruthenium(II): Factors governing binding to DNA. *J. Am. Chem. Soc.* **1989**, *111*, 3051–3058.
45. Xing, R.; Yu, H.; Liu, S.; Zhang, W.; Zhang, Q.; Li, Z.; Li, P. Antioxidant activity of differently regioselective chitosan sulfates in vitro. *Bioorg. Med. Chem.* **2005**, *13*, 1387–1392.